Clinical Ophthalmology

Dovepress
open access to scientific and medical research

Open Access Full Text Article

ORIGINAL RESEARCH

Comparison of choroidal neovascularization secondary to white dot syndromes and age-related macular degeneration by using optical coherence tomography angiography

This article was published in the following Dove Press journal:
Clinical Ophthalmology

Jay C Wang
Kenneth M McKay
Arjun B Sood
Inês Laíns
Lucia Sobrin
John B Miller

Retina Service, Department of Ophthalmology, Massachusetts Eye and Ear, Harvard Medical School, Boston, MA 02114, USA

Purpose: To characterize and compare choroidal neovascularization (CNV) secondary to white dot syndromes (WDS) and age-related macular degeneration (AMD) using optical coherence tomography angiography (OCT-A).

Methods: This is a cross-sectional study in which we imaged patients with CNV secondary to WDS and AMD with either the Zeiss Angioplex OCT-A or Optovue AngioVue OCT-A. Relevant demographic and clinical characteristics were collected and analyzed. CNV area and vessel density (VD) were measured by three independent graders, and linear regression analysis was subsequently performed.

Results: Three patients with multifocal choroiditis and panuveitis, one patient each with birdshot chorioretinopathy, presumed ocular histoplasmosis syndrome, and persistent placoid maculopathy, and eleven patients with AMD with sufficient image quality were included. CNV associated with WDS was significantly smaller than that secondary to AMD (0.56±0.32 vs 2.79±1.80 mm^2, β=–2.22, P=0.01), while no difference in VD was detected (0.46±0.09 vs 0.44±0.09, β=0.02, P=0.71).

Conclusion: CNV networks secondary to WDS appear to be smaller than those secondary to AMD but have similar VD. OCT-A is a powerful tool to investigate properties of CNV from various etiologies. Larger studies are needed for further characterization and understanding of CNV pathogenesis in inflammatory conditions.

Keywords: white dot syndromes, age-related macular degeneration, choroidal neovascularization, optical coherence tomography angiography, uveitis, inflammation, choroidal neovascular membrane

Plain language summary

Vision loss from age-related macular degeneration (AMD) and various inflammatory conditions of the retina is often due to the development of abnormal blood vessels beneath the retina. These blood vessels originate from the choroid and are termed choroidal neovascularization (CNV). However, how this process occurs in these conditions is poorly understood. In this study, we utilize a newer noninvasive imaging method called optical coherence tomography angiography to visualize CNV. We compared the characteristics of these vessels in AMD and inflammatory conditions of the retina. We found that when the CNV is due to inflammation, it is smaller in size and more focal than that from AMD, although the density of the vessels did appear to be similar. These results suggest that the cause of CNV in various inflammatory conditions of the retina may be distinct from that in AMD. This area certainly deserves further study and may lead to distinct treatments of CNV in the future.

Correspondence: John B Miller
Retina Service, Department of Ophthalmology, Massachusetts Eye and Ear, Harvard Medical School, 243 Charles Street, Boston, MA 02114, USA
Tel +1 617 573 3750
Fax +1 617 573 3698
Email john_miller@meei.harvard.edu

submit your manuscript | www.dovepress.com
Dovepress
http://dx.doi.org/10.2147/OPTH.S185468

Introduction

Choroidal neovascularization (CNV) is a process by which abnormal blood vessels proliferate in response to angiogenic stimuli and can be classified into numerous types depending on anatomic location and patterns of leakage.[1] CNVs are classically associated with exudative age-related macular degeneration (AMD).[2] However, they can also occur in posterior uveitis such as multifocal choroiditis and panuveitis (MCP), birdshot chorioretinopathy (BSCR), and presumed ocular histoplasmosis syndrome (POHS).[3] Anti-vascular endothelial growth factor (anti-VEGF) therapy is effective in reducing vascular leakage and improving vision in exudative AMD.[4] However, there is comparatively little experience with anti-VEGF therapy for CNV related to posterior uveitis and the pathophysiology of CNV in these entities is not completely understood.

The development of optical coherence tomography angiography (OCT-A) has enabled three-dimensional, non-invasive, high-resolution visualization of the retinal vasculature. While it cannot yet supplant fluorescein angiography (FA) or indocyanine green angiography (ICGA) in investigating choroidal pathology, it can be used in certain situations such as detecting CNV in cases where FA or ICGA is indeterminate or equivocal and distinguishing inflammatory lesions from CNV in white dot syndromes (WDS).[5–7] Using OCT-A, distinctive vessel morphologies have been identified in different types of CNV[8–10] and there are changes in vascular microarchitecture in response to anti-VEGF that have led to insights into the pathophysiology of CNV in AMD.[11,12]

A recent study suggested that CNV secondary to MCP appeared smaller and more well circumscribed than CNV secondary to AMD, suggesting a unique phenotype with implications for distinct pathogenesis.[13] A case report of CNV related to POHS also showed a small well-circumscribed appearance on OCT-A.[14] OCT-A characterization of CNV related to BSCR and persistent placoid maculopathy (PPM) has not been previously described. Here, we present a study of patients with CNV related to POHS, BSCR, PPM, and MCP with multimodal imaging, including longitudinal spectral domain OCT-A, and compare the features of these CNVs with those secondary to AMD.

Methods

Study design and protocol

This study was approved by the institutional review board (IRB) at Massachusetts Eye and Ear (MEE) and conformed to the provisions of the Declaration of Helsinki. All subjects provided written informed consent, which included the publication of data.

An existing imaging protocol is in place at our institution whereby patients with chorioretinal disease may be imaged with OCT-A with either the Zeiss Angioplex OCT-A (Carl Zeiss Meditec AG, Jena, Germany) or Optovue AngioVue OCT-A (Optovue, Fremont, CA, USA) on the 3×3 mm protocol. We reviewed this database and identified patients with a clinical diagnosis of CNV secondary to either posterior uveitis or AMD imaged from February 2016 to July 2017. Patients with infectious posterior uveitis, idiopathic posterior uveitis, or fewer than 6-month follow-up were excluded. The OCT-A images were reviewed, and after excluding those with poor image quality or equivocal findings (n=3), one patient each with POHS, BSCR, and PPM and three patients with MCP were included in this study. Simultaneously, 11 eyes of 11 patients with a diagnosis of exudative AMD imaged with OCT-A were also included for comparison. When both eyes had evidence of CNV, one was chosen at random for analysis.

Medical records were reviewed to collect demographic and clinical characteristics, including age, gender, diagnosis, presenting visual acuity, and imaging from ancillary studies, such as optical coherence tomography (OCT), FA, and fundus autofluorescence (FAF). The type of CNV was determined in each case on the basis of multimodal imaging, according to previously proposed criteria.[1] OCT-A images were viewed and exported using the built-in review software of Zeiss Angioplex and Optovue AngioVue. Manual adjustment of segmentation lines was performed whenever automatic segmentation was deemed to be inaccurate.

Image analysis

Measurement of CNV area and vessel density (VD) was performed in ImageJ (NIH, Bethesda, MD, USA) by three masked independent investigators (JCW, KMM, and ABS). The choriocapillaris slabs from both Zeiss Angioplex and Optovue Angiovue were utilized for analysis because the segmentation of this layer was found to be more robust and reliable than segmentation of the outer retinal layers, especially in the presence of intraretinal and subretinal fluid, even after manual adjustment. The polygon selection tool was used to manually outline the CNV network and saved as a region of interest (ROI). The entire image was then converted to 8 bit and binarized using the function adjust > threshold and the Otsu algorithm. The ROI was then reselected, and the area and VD were subsequently determined by the function analyze > measure. The measurements from the three independent graders were averaged. If the average difference was greater than 20%, the image was adjudicated by a fourth expert grader (JBM).

Statistical analysis

The study population demographics and clinical characteristics were summarized with traditional descriptive methods. Interclass correlation coefficient (ICC) was calculated for the CNV area and VD to assess the degree of agreement among the three graders. Additionally, paired *t*-tests were performed to compare CNV area and VD of eyes with WDS before and after anti-VEGF injection.

Using linear regression models, our statistical approach was centered on CNV area and VD. We started with univariate analyses for potential covariates and all parameters with a *P*-value of ≤0.25, and those with hypothesized clinical relevance were included in the initial multivariate models. A backward (step-down) elimination procedure was then used to achieve the multivariate models presented for CNV area and VD.

All statistics were performed using Stata® Version 12.1 (StataCorp LP, College Station, TX, USA), and *P*-values ≤0.05 were considered statistically significant.

Results

Case summaries

Case 1 (POHS)

A 67-year-old woman presented to MEE for the evaluation of POHS with recurrent CNV of the right eye. She received multiple intravitreal injections of bevacizumab at an outside institution over the past few years, and other etiologies of her condition were excluded via serological investigation. On presentation, her visual acuity was 20/20 in both eyes with normal IOPs. Fundus examination was consistent with bilateral POHS. In the right eye, a subfoveal elevation related to CNV was noted (Figure 1A). FA showed mild perifoveal leakage (Figure 1B). Structural OCT revealed subfoveal fluid in the right eye with pigment epithelial detachments (Figure 1C). Photodynamic therapy (PDT) was added to her regimen with improved response, and the patient is now maintained on monthly injections of aflibercept.

OCT-A was performed during a recurrence (Figure 1D) and showed a moderate amount of subretinal fluid with no obvious CNV. We treated the patient with the combination of PDT and anti-VEGF with complete resolution of subretinal fluid at the last follow-up (Figure 1E). As the amount of subretinal fluid decreased, the CNV became more clearly visible on OCT-A and is demonstrated by a network of tortuous and looping vascular structures in the choriocapillaris slab.

Case 2 (BSCR)

A 58-year-old woman was referred to MEE for the management of BSCR complicated by CNV of the right eye. She received intravitreal bevacizumab (1.25 mg/0.05 mL) injection 1 month prior. On presentation, her visual acuity was 20/40 in the right eye and 20/25 in the left eye with normal IOPs. Dilated fundus examination showed mild vitritis in both eyes and multiple ovoid hypopigmented lesions throughout both retinae, as well as two hypopigmented lesions inferior to the fovea in the right eye (Figure 2A). FA revealed multiple

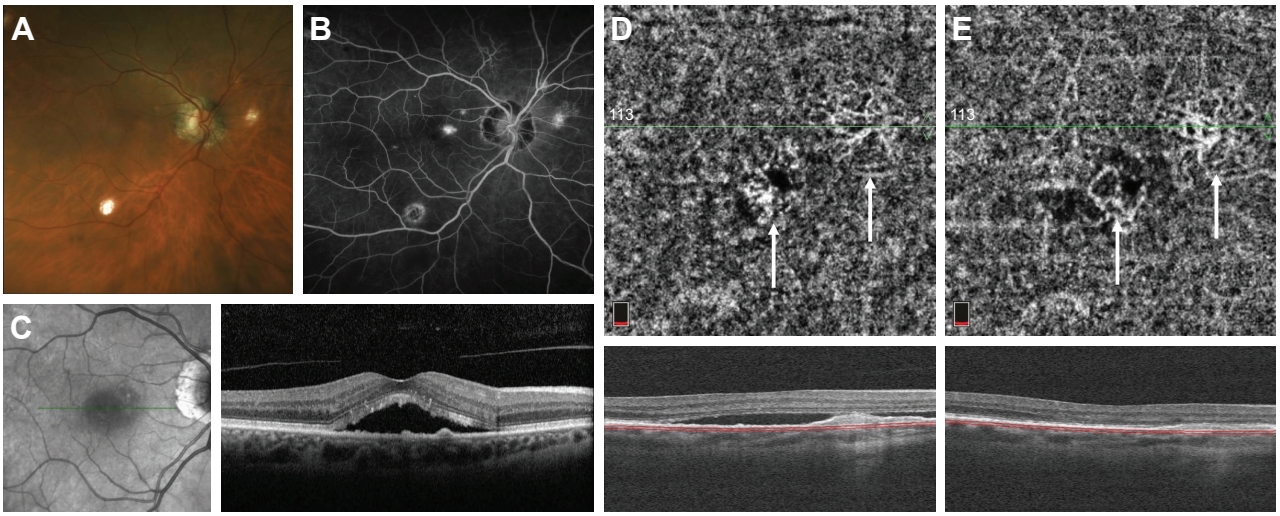

Figure 1 Fundus photograph of the right eye with POHS showing peripapillary atrophy and multiple "punched out" chorioretinal scars (**A**). Late-phase fluorescein angiogram demonstrating a small area of hyperfluorescence at the fovea (**B**). Structural OCT on initial presentation showing subretinal fluid and multiple small pigment epithelial detachments (**C**). OCT-A of the choriocapillaris obtained during a recurrence of subretinal fluid after multiple anti-VEGF injections demonstrates two areas of branching CNV networks (white arrows) (**D**). After anti-VEGF injection, the subretinal fluid is resolved and the CNV networks become more clearly visualized (**E**).

Abbreviations: Anti-VEGF, anti-vascular endothelial growth factor; CNV, choroidal neovascularization; OCT-A, optical coherence tomography angiography; POHS, presumed ocular histoplasmosis syndrome.

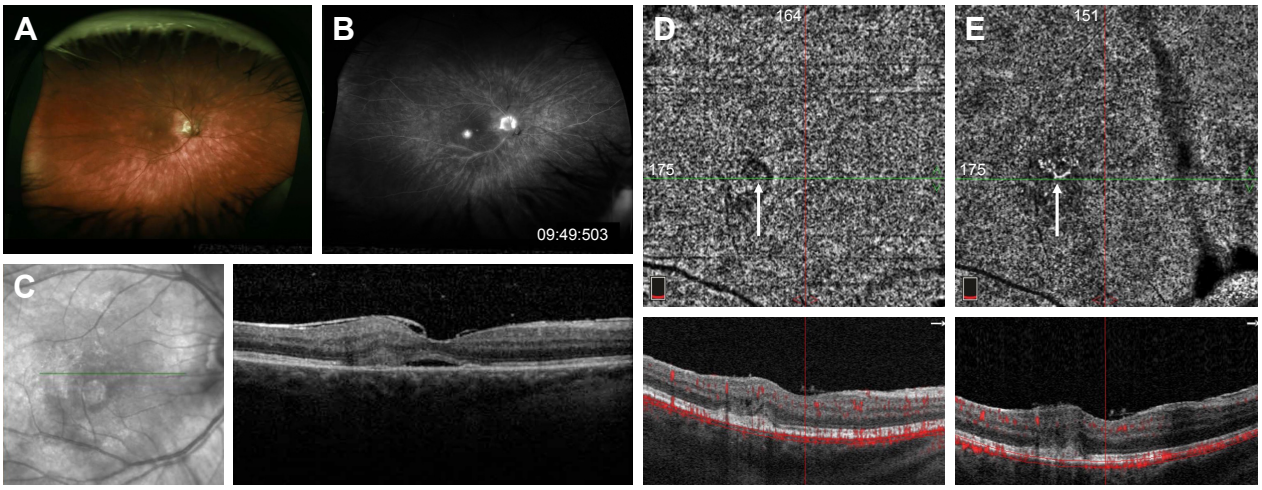

Figure 2 Fundus photograph of the right eye with BSCR showing multiple ovoid hypopigmented lesions in the mid-periphery (**A**). Late-phase fluorescein angiogram demonstrating an area of more intense hyperfluorescence at the fovea (**B**). Structural OCT on initial presentation showing subretinal fluid and adjacent subretinal hyper-reflective material (**C**). After multiple anti-VEGF injections, the subretinal fluid is resolved and, on OCT-A of the choriocapillaris, there is only a very faint area of flow signal surrounded by a halo of decreased signal (**D**). Twelve months later without anti-VEGF injections, OCT-A shows a clearer branching CNV network but still without any subretinal fluid (**E**).
Abbreviations: Anti-VEGF, anti-vascular endothelial growth factor; BSCR, birdshot chorioretinopathy; CNV, choroidal neovascularization; OCT-A, optical coherence tomography angiography.

areas of vascular leakage and intense leakage just inferior to the fovea of the right eye (Figure 2B). On structural OCT, subretinal hyperreflective material with associated subretinal fluid was observed in the area corresponding to leakage consistent with CNV (Figure 2C). The patient was started on mycophenolate mofetil and cyclosporine. After multiple intravitreal injections of aflibercept, the subretinal fluid is resolved, leaving only chronic cystic changes in the retina a year later. OCT-A at that point showed an area of faint flow signal in the choriocapillaris layer surrounded by a halo of decreased signal (Figure 2D). Follow-up OCT-A 12 months later without anti-VEGF injections shows a clearer branching CNV network but still without any subretinal fluid (Figure 2E).

Case 3 (MCP)

A 38-year-old woman was presented to MEE with several days of blurry vision and metamorphopsia of the left eye. Her visual acuity was 20/20 in the right eye and 20/40 in the left eye with normal IOPs. Ophthalmological examination showed an area of mild elevation in the macula and several chorioretinal scars in the nasal retina of the left eye without vitritis (Figure 3A). FA revealed window defects corresponding to the chorioretinal scars and early hyperfluorescence with intense late leakage at the fovea consistent with CNV (Figure 3B). Structural OCT demonstrated subretinal hyperreflective material with disruption of the outer retinal layers and adjacent subretinal fluid (Figure 3C). OCT-A

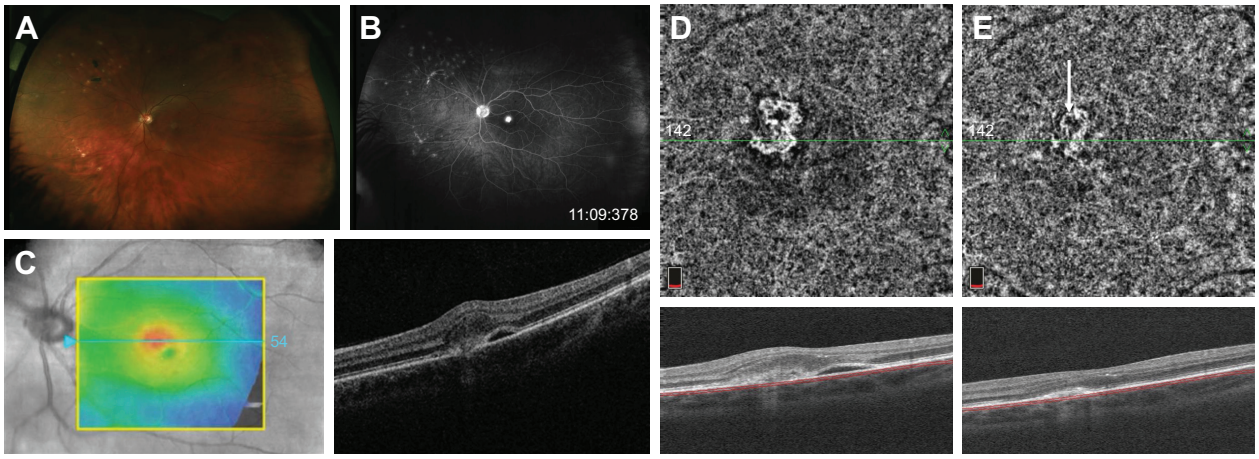

Figure 3 Fundus photography of the left eye with MCP showing multiple "punched out" chorioretinal scars in the periphery (**A**). Late-phase fluorescein angiogram demonstrating a discrete area of intense hyperfluorescence at the fovea (**B**). Structural OCT on initial presentation showing subretinal fluid and adjacent subretinal hyper-reflectivity (**C**). OCT-A of the choriocapillaris demonstrates a clear well-circumscribed CNV network (**D**), which diminishes in size and intensity after anti-VEGF injection (**E**).
Abbreviations: Anti-VEGF, anti-vascular endothelial growth factor; CNV, choroidal neovascularization; MCP, multifocal choroiditis and panuveitis; OCT-A, optical coherence tomography angiography.

clearly showed a well-circumscribed looped CNV network in the choriocapillaris slab (Figure 3D). After an investigation for underlying etiologies, she was diagnosed with idiopathic MCP with CNV, started on oral prednisone, and received an intravitreal injection of bevacizumab. On follow-up examination 1 month later, her visual acuity improved to 20/25, structural OCT showed the resolution of subretinal fluid, and OCT-A demonstrated a smaller, less dense CNV network though an outer anastomotic ring remains (Figure 3E).

Case 4 (MCP)

A 53-year-old woman was referred to MEE for the evaluation of recurrent episodes of vitritis and subretinal fluid. She had not received any prior intravitreal anti-VEGF injections. On presentation, her visual acuity was 20/50 in the right eye and 20/20 in the left eye with normal IOPs. Dilated fundus examination showed mild vitritis, peripapillary atrophy, and multiple hypopigmented punched out lesions in the periphery of both eyes. A peripapillary subretinal lesion with greenish hue and associated subretinal fluid was also present in the right eye (Figure 4A). FA showed early peripapillary hyperfluorescence with intense late leakage in the right eye corresponding to the lesion seen clinically (Figure 4B). Structural OCT also confirmed the presence of subretinal fluid with numerous intraretinal exudates and a large mound of subretinal hyperreflectivity (Figure 4C).

An investigation for an underlying etiology was unrevealing. The patient was started on a taper of oral prednisone at this time, which briefly resulted in the resolution of the subretinal fluid, but it recurred after the cessation of steroid therapy. She started on mycophenolate mofetil but without complete resolution of subretinal fluid. Structural OCT 3 months later showed some persistent but improved intraretinal fluid, and OCT-A more clearly showed the network of CNV in the peripapillary region (Figure 4D). She then proceeded to receive four monthly injections of aflibercept with some improvement in vision. Structural OCT at the most recent follow-up 2 months after the last injection showed only minimal intraretinal fluid, and the CNV appeared smaller and less dense on OCT-A with some surrounding regions of decreased flow signal in the choriocapillaris (Figure 4E).

Case 5 (MCP)

A 64-year-old man was returned in follow-up to MEE for CNV secondary to multifocal choroiditis in both eyes diagnosed 8 years prior. His choroiditis was felt to be secondary to acute disseminated encephalomyelitis.[15] His right eye was randomly chosen for analysis. He had received many intravitreal injections of ranibizumab and aflibercept in both eyes. On presentation, his visual acuity was 20/63 in the right eye and counting fingers in the left eye with normal IOPs. Dilated fundus examination showed subretinal fibrosis in both eyes, with hypoautofluorescence (Figure 5A and B). Structural OCT demonstrated subretinal hyperreflectivity with minimal subretinal fluid (Figure 5C). OCT-A showed a looping vascular network in the superior macula consistent with CNV (Figure 5D). The patient was treated with an intravitreal injection of aflibercept.

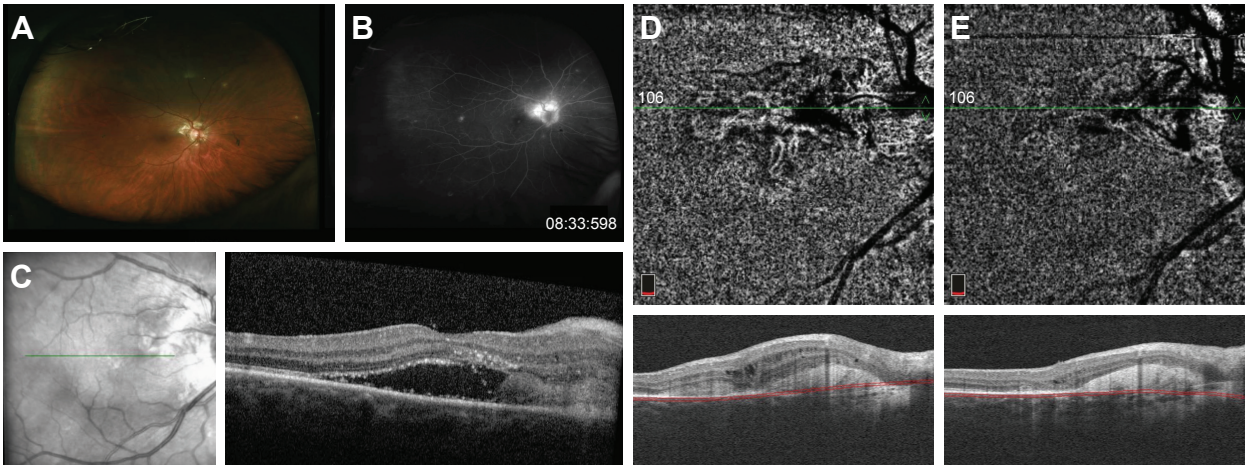

Figure 4 Fundus photography of the right eye with MCP showing a mildly elevated peripapillary subretinal lesion (**A**). Late-phase fluorescein angiogram demonstrating intense peripapillary hyperfluorescence corresponding to the subretinal lesion seen on fundus examination (**B**). Structural OCT on initial presentation showing subretinal fluid with an adjacent area of subretinal hyper-reflectivity (**C**). Interval improvement in subretinal fluid after initiation of oral steroid and steroid-sparing immunosuppressive therapy and OCT-A of the choriocapillaris demonstrates a branching CNV network extending from the optic nerve toward the macula (**D**). After initiation of anti-VEGF therapy, the CNV is less well visualized and diminished in both area and intensity (**E**).

Abbreviations: Anti-VEGF, anti-vascular endothelial growth factor; CNV, choroidal neovascularization; MCP, multifocal choroiditis and panuveitis; OCT-A, optical coherence tomography angiography.

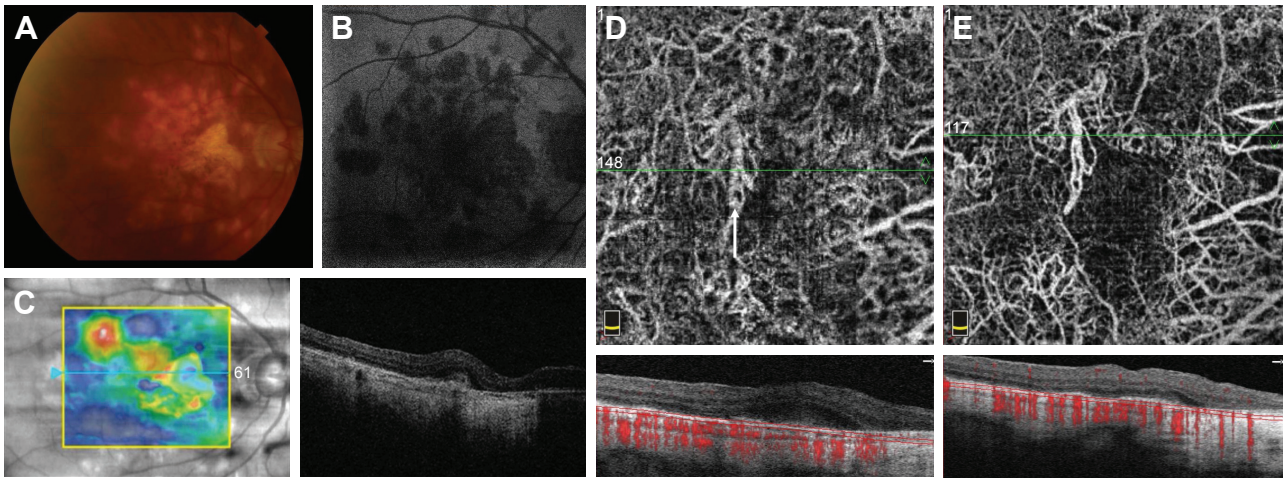

Figure 5 Fundus photography of the right eye with MCP showing multiple areas of chorioretinal atrophy centrally (**A**). Autofluorescence demonstrating hypoautofluorescense in these areas (**B**). Structural OCT showing subretinal hyper-reflectivity and associated subretinal fluid (**C**). OCT-A of the choriocapillaris demonstrates a looping anastamotic vascular network (arrow) (**D**), which becomes more clearly delineated after anti-VEGF injection with the resolution of subretinal fluid (**E**).
Abbreviations: Anti-VEGF, anti-vascular endothelial growth factor; MCP, multifocal choroiditis and panuveitis; OCT-A, optical coherence tomography angiography.

Three months later, his vision improved to 20/32 in the right eye. Structural OCT demonstrated subretinal hyperreflectivity without subretinal fluid. OCT-A again showed the vascular looping networks consistent with CNV (Figure 5E).

Case 6 (PPM)

A 64-year-old woman was returned in follow-up to MEE for CNV secondary to PPM in both eyes, diagnosed many years prior after a negative investigation for underlying diseases, with a new complaint of decreased vision in the left eye. Her left eye was randomly chosen for analysis. She had been receiving regular intravitreal injections of aflibercept in both eyes. She had also undergone implantation of the 0.59 mg fluocinolone acetonide implant (Retisert) in both eyes 3 years prior. On presentation, her visual acuity was 20/32 in the right eye and 20/40 in the left eye with normal IOPs. Dilated fundus examination showed a new area of subretinal fibrosis inferior to the fovea in the left eye with stippled hypo- and hyperautofluorescence (Figure 6A and B). Structural OCT demonstrated a new area of subretinal hyperreflectivity without subretinal fluid inferior to the fovea (Figure 6C). OCT-A showed an abnormal vascular network around the fovea of the left eye (Figure 6D). The patient was treated with her scheduled intravitreal injection of aflibercept as

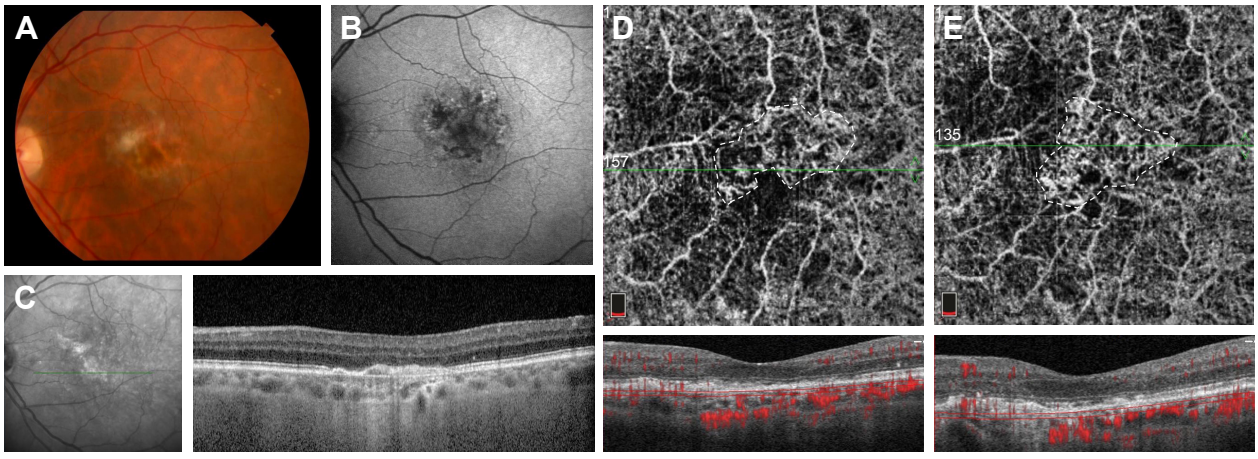

Figure 6 Fundus photography of the left eye with PPM showing chorioretinal atrophy and subretinal fibrosis (**A**). Autofluorescence demonstrating stippled hypo and hyperautofluorescense centrally (**B**). Structural OCT showing subretinal hyper-reflectivity without associated subretinal fluid (**C**). OCT-A of the choriocapillaris demonstrates a branching vascular network (outlined by dashed line) (**D**) which is redemonstrated after anti-VEGF injection (outlined by dashed line) (**E**).
Abbreviations: Anti-VEGF, anti-vascular endothelial growth factor; OCT-A, optical coherence tomography angiography; PPM, persistent placoid maculopathy.

well as 0.4 mg triamcinolone acetonide due to the concern for possible recurrent choroiditis.

Two months later, her vision improved to 20/25 in the left eye. Structural OCT demonstrated a decrease in the area of subretinal hyperreflectivity without subretinal fluid inferior to the fovea. OCT-A again showed an abnormal vascular network around the fovea of the left eye (Figure 6E).

Summary of CNV characteristics in WDS and AMD

Table 1 summarizes the relevant imaging characteristics of CNV in the above cases of WDS, including CNV type, area, and VD. Qualitatively, most of the CNV networks appeared small, focal, well circumscribed, and globular in shape (cases 1–3). However, morphology with central branching or larger vessels and peripheral looping/anastomoses of smaller vessels was also observed and these lesions tended to be larger (cases 4–6).

A decrease in both CNV area and VD was seen in treatment-naive cases (3 and 4) after anti-VEGF therapy. In other cases, an increase in either CNV area or VD was observed. Paired *t*-tests comparing overall CNV area and VD before and after anti-VEGF treatment were not statistically significant (P=0.98 and 0.59, respectively).

Table 2 compares demographic, clinical, and relevant imaging variables for the WDS and AMD patients considered in this study. There was excellent inter-grader reliability – the ICC for CNV area and VD was 0.99 and 0.85, respectively. The average CNV area in WDS was 0.56±0.32 mm^2, and that in AMD was 2.79±1.80 mm^2 (P=0.01). The average CNV VD in WDS was 0.46±0.09, and that in AMD was 0.44±0.09 (P=0.71).

Representative OCT-A images at the choriocapillaris of various CNV structures in exudative AMD are shown in Figure 7.

Univariate analyses

Results of univariate analyses for CNV area and VD are shown in Table 3. For CNV area, a statistically significant association was observed with age, number of prior injections, and diagnosis (AMD vs WDS) ($P \leq 0.03$). CNV type (1 vs 2) and OCT-A platform (Zeiss vs Optovue) were borderline significant. For CNV VD, only the type of OCT-A platform (Zeiss vs Optovue) used and prior PDT presented a significant association (P=0.04, for both).

Multivariate analyses

As described in the "Methods" section, we used backward elimination procedures for multivariate analyses. For CNV area, the best model (adjusted R^2=0.46) demonstrated that higher number of prior injections (β=0.07, P=0.05) and AMD diagnosis (β=1.88, P=0.02) were significantly associated with larger CNV areas. For VD, the best model (adjusted R^2=0.67) included OCT-A platform (Zeiss vs Optovue) (β=0.23, $P<0.001$), months since last injection (β=0.002, P=0.02), presence of subretinal fluid (β=–0.06, P=0.04), and age (β=0.01, P=0.004). However, diagnosis (AMD vs WDS) was not a significant predictor of VD.

Discussion

In this study, we utilized spectral domain OCT-A to characterize CNV in various WDS, including POHS, BSCR, PPM, and MCP, and compared them to CNV secondary to AMD. We also demonstrated longitudinal changes in CNV

Table 1 Summary of imaging characteristics of CNV associated with inflammatory chorioretinopathies

Case	Disease	Eye	OCT-A modality	Number of previous anti-VEGF injections	Time since last injection (months)	PDT	CNV type	Before anti-VEGF		After anti-VEGF	
								CNV area (mm^2)	CNV vessel density	CNV area (mm^2)	CNV vessel density
1	POHS	OD	Optovue	10 bevacizumab, 22 aflibercept	0.5	Yes	1	0.71	0.48	1.01	0.48
2	BSCR	OD	Optovue	2 bevacizumab, 4 aflibercept	6	No	2	0.12	0.34	–	–
3	MCP	OS	Optovue	None	–	No	2	0.27	0.60	0.17	0.53
4	MCP	OD	Optovue	None	–	No	2	0.58	0.42	0.31	0.34
5	MCP	OD	Optovue	5 randibizumab, 28 aflibercept	2	No	2	0.98	0.43	0.71	0.50
6	PPM	OS	Optovue	5 aflibercept	0.5	No	2	0.72	0.47	1.04	0.47

Abbreviations: anti-VEGF, anti-vascular endothelial growth factor; BSCR, birdshot chorioretinopathy; CNV, choroidal neovascularization; MCP, multifocal choroiditis and panuveitis; OCT-A, optical coherence tomography angiography; PDT, photodynamic therapy; POHS, presumed ocular histoplasmosis syndrome; PPM, persistent placoid maculopathy.

Table 2 Summary of demographic and clinical characteristics for eyes with CNV due to AMD and WDS

	AMD	WDS	*P*-value
Age (years)	77.3±8.1	58.3±11.3	0.001
% female	64% (7/11)	83% (5/6)	0.42
% OD	45% (5/11)	67% (4/6)	0.40
% Zeiss	36% (4/11)	0% (0/6)	0.10
Number of prior injections	16.2±9.7	11±13.5	0.37
Months since last injection	12.7±21.2	2.25±2.6	0.25
LogMAR VA	0.32±0.26	0.27±0.16	0.43
% with SRF	64% (7/11)	67% (4/6)	0.90
% with prior PDT	27% (3/11)	17% (1/6)	0.65
% CNV Type 1	73% (8/11)	17% (1/6)	0.03
CNV area (mm^2)	2.79±1.80	0.56±0.32	0.01
CNV vessel density	0.44±0.09	0.46±0.09	0.71

Abbreviations: AMD, age-related macular degeneration; CNV, choroidal neovascularization; logMAR VA, logarithm of the minimum angle of resolution visual acuity; PDT, photodynamic therapy; SRF, subretinal fluid; WDS, white dot syndromes.

architecture with anti-VEGF therapy in WDS. In general, CNV networks secondary to WDS seem to be smaller but have similar VD. There was an association between number of prior injections and larger CNV size, which may simply be a reflection that larger CNV lesions are more difficult to treat and require more anti-VEGF injections.

Distinct CNV morphologies have been observed using OCT-A. For instance, the morphology of Type 1 CNV is characterized by large networks with dilated core feeder vessels described as "medusa-like" or "sea-fan shaped", with an average area of greater than 5 mm^2.[16] Type 2 CNV lesions tend to be well circumscribed, often "glomerulus" like in appearance with a surrounding dark ring of attenuated signal.[17] In one recent study directly comparing Type 1 and Type 2 CNV, Type 2 CNV was found to be smaller on average with more well-defined borders.[18] The activity of these lesions may also be predicted by certain characteristics on OCT-A, such as a well-defined shape with branching, anastomoses and loops, and the presence of a perilesional hypointense halo.[19]

Reductions in the size and VD of CNV networks have been shown for treatment-naive lesions in both Type 1 and Type 2 CNV,[12] but it appears that chronic lesions do not demonstrate significant changes with repeated injections and, instead, adopt a more stable mature "filamentous" or "loose-net" configuration with larger central vessels.[20,21] The underlying mechanism for this transformation is thought to be related to the process of arteriogenesis and pruning of smaller peripheral capillaries with repeated anti-VEGF therapy.[11] In between anti-VEGF injections, however, smaller peripheral capillaries redevelop. Our finding of increasing VD with increasing time since last injection is consistent with this hypothesis.

The current literature on the OCT-A characteristics of CNV in MCP has identified both Type 1 and Type 2 lesions.[13,22–24] Overall, it appears that these lesions are generally less than 1 mm^2 in area and are fairly well circumscribed, often with a halo of decreased signal.[13,22,25] All three cases of CNV in MCP in our study were Type 2 lesions, one of which (Case 3) appeared very well circumscribed and could be

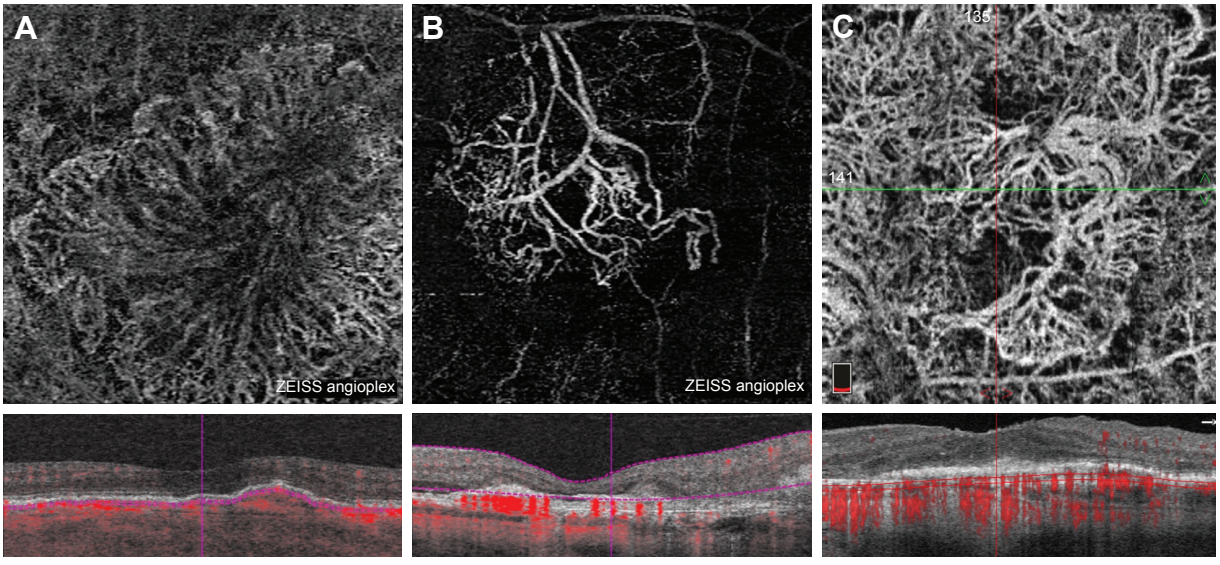

Figure 7 Representative OCT-A images at the level of the choriocapillaris of patients with exudative AMD from Table 2.
Notes: Large "medusa" like CNV network in an eye having received multiple prior anti-VEGF injections (**A**). Large branching CNV network in an eye having received multiple prior anti-VEGF injections (**B**). Large "seafan" like CNV network in an eye having received multiple prior anti-VEGF injections (**C**).
Abbreviations: AMD, age-related macular degeneration; anti-VEGF, anti-vascular endothelial growth factor; CNV, choroidal neovascularization; OCT-A, optical coherence tomography angiography.

Table 3 Univariate regression analysis of CNV area (mm^2) and vessel density

Variables	CNV area (mm^2)			CNV vessel density		
	β coefficient	95% CI	*P*-value	*β* coefficient	95% CI	*P*-value
Age	0.09	0.03 to 0.15	0.004	−0.002	−0.01 to 0.002	0.30
Gender	0.43	−1.7 to 2.5	0.67	0.01	−0.09 to 0.11	0.84
Eye (OD vs OS)	−0.38	−2.3 to 1.5	0.67	0.06	−0.03 to 0.15	0.15
OCT-A platform (Zeiss vs Optovue)	−1.82	−3.9 to 0.2	0.08	0.10	0.004 to 0.20	0.04
Number of prior injections	0.09	0.01 to 0.16	0.03	−0.002	−0.01 to 0.002	0.29
Months since last injection	−0.03	−0.08 to 0.03	0.34	0.001	−0.001 to 0.004	0.36
LogMAR VA	0.92	−3.5 to 5.3	0.66	0.03	−0.19 to 0.24	0.81
Presence of subretinal fluid	0.24	−1.8 to 2.3	0.80	−0.0002	−0.1 to 0.1	0.99
Prior PDT	0.46	−1.8 to 2.7	0.67	−0.10	−0.20 to −0.01	0.04
CNV type (1 vs 2)	−1.60	−3.3 to 0.12	0.07	−0.05	−0.14 to 0.05	0.31
Diagnosis (AMD vs WDS)	−2.22	0.6 to 3.8	0.01	0.02	−0.12 to 0.08	0.71

Note: 95% CIs and *P*-values are for the *β* coefficient.
Abbreviations: AMD, age-related macular degeneration; CNV, choroidal neovascularization; logMAR VA, logarithm of the minimal angle of resolution visual acuity; OCT-A, optical coherence tomography angiography; PDT, photodynamic therapy; WDS, white dot syndromes.

described as "glomerulus like", similar to what has previously been described in Type 2 lesions of exudative AMD.[17] The other cases (Cases 4 and 5) were slightly larger and exhibited a central branching with peripheral looping/anastomotic pattern. These lesions were smaller even when compared with similar Type 2 lesions in AMD.

Clinically, it has been shown that anti-VEGF therapy for CNV in MCP is efficacious in improving visual acuity.[26] However, significant changes in the size or appearance of CNV on OCT-A are not always observed. Only in lesions that are treatment naive are reductions in CNV area and VD observed after anti-VEGF treatment.[13,24] In this study, both treatment-naive lesions in MCP demonstrated reductions in CNV area and VD in response to anti-VEGF therapy.

A case of treatment-naive CNV in POHS was recently characterized with OCT-A, which was small and well circumscribed, and appeared to decrease in size with initial anti-VEGF therapy.[14] However, with repeated anti-VEGF therapy, no further decrease in size is observed. Our case of CNV in POHS was similarly small and well circumscribed but not treatment naive. Anti-VEGF therapy led to increases in CNV area on OCT-A without changes in VD. However, we theorize that the resolution of subretinal fluid with anti-VEGF therapy allowed better penetration of optical signal and visualization of residual CNV. Though this may have also occurred with our treatment-naive lesions, the amount of subretinal fluid to begin with in these cases was minimal and more substantial regression of the CNV network was likely, given the lack of previous anti-VEGF exposure.

Though CNV in PPM and BSCR has not previously been characterized by OCT-A, anti-VEGF therapy has been shown to improve visual acuity in these conditions and, in the case of BSCR, it is utilized along with systemic immunosuppression.[27,28] In this study, the CNV structure in PPM was of moderate size with an intricate network of branching vessels. This lesion was not anti-VEGF naive, and further therapy actually resulted in increases in CNV area on OCT-A without changes in VD. The CNV structure imaged in our case of BSCR was initially very small and faint on OCT-A but, despite becoming more well-delineated over time, remained quiescent without requiring anti-VEGF therapy.

In our study, we observed that the size of CNV lesions from WDS was smaller and more focal than CNV from exudative AMD. This may have implications for our understanding of the pathogenesis of these conditions. It is thought that inflammation plays a significant role in the formation of CNV in AMD, as it has been shown that inflammatory cells and VEGF co-localize in animal models of CNV and that steroids can effectively treat CNV in some of these models.[29,30] It is perhaps not surprising then that both AMD and WDS can lead to CNV. However, the difference in size and appearance of CNV may be a reflection of the more focal nature of inflammation in WDS, such as in MCP and POHS, which contrasts with the more diffuse macular process of AMD. We observed Type 2 CNV networks in MCP, BSCR, and PPM, which may be explained by inflammatory damage to Bruch's membrane allowing neovessels to proliferate in the subretinal space. In contrast, the Type 1 CNV seen in POHS could be a result of deeper choroidal seeding of *Histoplasma capsulatum* spores sparing Bruch's membrane.

OCT-A has become a powerful tool for the visualization of CNV networks, and especially in WDS, it has the

potential to distinguish active inflammatory deposits that may mimic active CNV on FA and structural OCT, from actual CNV.[13,23,24,31] However, meaningful interpretation of OCT-A images requires cautious analysis. Accurate segmentation is especially crucial in these cases because subretinal hyperreflectivity, pigment epithelial detachments, subretinal fluid, and intraretinal fluid are often present and can lead to inaccurate automated segmentation of the retinal layers. Even when segmentation is performed accurately, the presence of subretinal hemorrhage can attenuate signal from deeper layers of the choriocapillaris and choroid and lead to the inability to visualize CNV.[6] In our experience, it also appears that a large amount of subretinal fluid can also have a similar effect, which can potentially limit the sensitivity of OCT-A for CNV in patients who are newly diagnosed. We did find that the presence of subretinal fluid was significantly associated with decreased VD. It is notable that in the published literature of OCT-A in treatment-naive CNV, structural OCT shows little to no subretinal fluid.[12] Other image artifacts can also occur, including projection artifacts, subthreshold blood flow, motion artifact, and attenuation of flow signal from overlying material, which are especially relevant in patients with inflammatory deposits.[32] Furthermore, the visualization of choroidal vessels in eyes with RPE atrophy may be confused with CNV.[33] Thus, any meaningful interpretation of OCT-A requires a multimodal imaging approach.

The strengths of this study include the use of multimodal imaging for the analysis of OCT-A images, manual adjustment of segmentation when necessary, consistent and reliable measurements of CNV area and VD among graders, comparison of CNV lesions to those in exudative AMD, and the demonstration of longitudinal changes with anti-VEGF therapy. In addition, we have utilized different OCT-A modalities for the characterization of CNV and we performed multivariate models to account for the influence of the different covariates on the assessment of our outcomes. One limitation of this study is the small number of patients; thus, while it is difficult to make definitive conclusions, our findings certainly highlight the need for further studies. In addition, it is possible that the CNV areas were larger in AMD because of longer duration of exudative disease, but even when controlling for this parameter, diagnosis was still a significant predictor. Although there were differences in the two groups in the proportion of eyes with Type 1 CNV, proportion of eyes treated, types of treatment, imaging modality used, and age, these variables were controlled for in the multivariable analysis. CNV networks from longstanding inflammatory disease were still significantly smaller.

Conclusion

Certainly, larger studies of CNV in WDS are needed for further characterization of these lesions and understanding whether observed differences in morphology in these lesions are clinically significant or meaningful. Despite its current technical limitations, OCT-A already provides a powerful tool for the morphological analysis of CNV lesions. Future technical advancements including the ability to image leakage will further add to its value in diagnosis and management.

Acknowledgment

This research received no specific grant from any funding agency in the public, commercially, or not-for-profit sectors.

Disclosure

The authors report no conflicts of interest in this work.

References

1. Freund KB, Zweifel SA, Engelbert M. Do we need a new classification for choroidal neovascularization in age-related macular degeneration? *Retina*. 2010;30(9):1333–1349.
2. Zarbin MA. Current concepts in the pathogenesis of age-related macular degeneration. *Arch Ophthalmol*. 2004;122(4):598.
3. Weber ML, Heier JS. Choroidal Neovascularization Secondary to Myopia, Infection and Inflammation. *Dev Ophthalmol*. 2016;55:167–175.
4. Dadgostar H, Waheed N. The evolving role of vascular endothelial growth factor inhibitors in the treatment of neovascular age-related macular degeneration. *Eye*. 2008;22(6):761–767.
5. Jia Y, Bailey ST, Hwang TS, et al. Quantitative optical coherence tomography angiography of vascular abnormalities in the living human eye. *Proc Natl Acad Sci U S A*. 2015;112(18):E2395–E2402.
6. de Carlo TE, Bonini Filho MA, Chin AT, et al. Spectral-domain optical coherence tomography angiography of choroidal neovascularization. *Ophthalmology*. 2015;122(6):1228–1238.
7. Wang JC, Laíns I, Sobrin L, Miller JB. Distinguishing white dot syndromes with patterns of choroidal hypoperfusion on optical coherence tomography angiography. *Ophthalmic Surg Lasers Imaging Retina*. 2017;48(8):638–646.
8. Iafe NA, Phasukkijwatana N, Sarraf D. Optical Coherence Tomography Angiography of Type 1 Neovascularization in Age-Related Macular Degeneration. *Dev Ophthalmol*. 2016;56:45–51.
9. Querques G, Miere A, Souied EH. Optical Coherence Tomography Angiography Features of Type 3 Neovascularization in Age-Related Macular Degeneration. *Dev Ophthalmol*. 2016;56:57–61.
10. Souied EH, El Ameen A, Semoun O, Miere A, Querques G, Cohen SY. Optical Coherence Tomography Angiography of Type 2 Neovascularization in Age-Related Macular Degeneration. *Dev Ophthalmol*. 2016;56:52–56.
11. Spaide RF. Optical Coherence Tomography Angiography Signs of Vascular Abnormalization With Antiangiogenic Therapy for Choroidal Neovascularization. *Am J Ophthalmol*. 2015;160(1):6–16.
12. Muakkassa NW, Chin AT, de Carlo T, et al. Characterizing the effect of anti-vascular endothelial growth factor therapy on treatment-naive choroidal neovascularization using optical coherence tomography angiography. *Retina*. 2015;35(11):2252–2259.
13. Cheng L, Chen X, Weng S, et al. Spectral-Domain Optical Coherence Tomography Angiography Findings in Multifocal Choroiditis With Active Lesions. *Am J Ophthalmol*. 2016;169:145–161.

14. Liu TYA, Zhang AY, Wenick A. Evolution of Choroidal Neovascularization due to Presumed Ocular Histoplasmosis Syndrome on Multimodal Imaging including Optical Coherence Tomography Angiography. *Case Rep Ophthalmol Med*. 2018;2018:1–5.
15. Panou N, Kim IK, Sobrin L. Choroiditis and choroidal neovascularization in acute disseminated encephalomyelitis. *Retin Cases Brief Rep*. 2013;7(1):89–90.
16. Kuehlewein L, Bansal M, Lenis TL, et al. Optical Coherence Tomography Angiography of Type 1 Neovascularization in Age-Related Macular Degeneration. *Am J Ophthalmol*. 2015;160(4):739–748.
17. El Ameen A, Cohen SY, Semoun O, et al. Type 2 neovascularization secondary to age-related macular degeneration imaged by optical coherence tomography angiography. *Retina*. 2015;35(11):2212–2218.
18. Farecki ML, Gutfleisch M, Faatz H, et al. Characteristics of type 1 and 2 CNV in exudative AMD in OCT-Angiography. *Graefes Arch Clin Exp Ophthalmol*. 2017;255(5):913–921.
19. Coscas GJ, Lupidi M, Coscas F, Cagini C, Souied EH. Optical coherence tomography angiography versus traditional multimodal imaging in assessing the activity of exudative age-related macular degeneration: a new diagnostic challenge. *Retina*. 2015;35(11):2219–2228.
20. Sulzbacher F, Pollreisz A, Kaider A, et al. Identification and clinical role of choroidal neovascularization characteristics based on optical coherence tomography angiography. *Acta Ophthalmol*. 2017;95(4):414–420.
21. Parravano M, Querques L, Scarinci F, et al. Optical coherence tomography angiography in treated type 2 neovascularization undergoing monthly anti-VEGF treatment. *Acta Ophthalmol*. 2017;95(5):e425–e426.
22. Zahid S, Chen KC, Jung JJ, et al. Optical coherence tomography angiography of chorioretinal lesions due to idiopathic multifocal choroiditis. *Retina*. 2017;37(8):1451–1463.
23. Levison AL, Baynes KM, Lowder CY, Kaiser PK, Srivastava SK. Choroidal neovascularisation on optical coherence tomography angiography in punctate inner choroidopathy and multifocal choroiditis. *Br J Ophthalmol*. 2017;101(5):616–622.
24. Baumal CR, de Carlo TE, Waheed NK, Salz DA, Witkin AJ, Duker JS. Sequential Optical Coherence Tomographic Angiography for Diagnosis and Treatment of Choroidal Neovascularization in Multifocal Choroiditis. *JAMA Ophthalmol*. 2015;133(9):1087.
25. Dutheil C, Korobelnik JF, Delyfer MN, Rougier MB. Optical coherence tomography angiography and choroidal neovascularization in multifocal choroiditis: A descriptive study. *Eur J Ophthalmol*. 2018;28(5):614–621.
26. Parodi MB, Iacono P, Kontadakis DS, Zucchiatti I, Cascavilla ML, Bandello F. Bevacizumab vs photodynamic therapy for choroidal neovascularization in multifocal choroiditis. *Arch Ophthalmol*. 2010;128(9):1100–1103.
27. Parodi MB, Iacono P, Bandello F. Juxtafoveal choroidal neovascularization secondary to persistent placoid maculopathy treated with intravitreal bevacizumab. *Ocul Immunol Inflamm*. 2010;18(5):399–401.
28. Shantha JG, Ho VY, Patel P, Forooghian F, Yeh S. Choroidal Neovascularization Associated With Birdshot Chorioretinopathy. *Ophthalmic Surg Lasers Imaging Retina*. 2016;47(5):450–457.
29. Nussenblatt RB, Ferris F. Age-related macular degeneration and the immune response: implications for therapy. *Am J Ophthalmol*. 2007;144(4):618–626.
30. Spaide RF. Rationale for combination therapies for choroidal neovascularization. *Am J Ophthalmol*. 2006;141(1):149–156.
31. Astroz P, Miere A, Mrejen S, et al. Optical coherence tomography angiography to distinguish choroidal neovascularization from macular inflammatory lesions in multifocal choroiditis. *Retina*. 2018;38(2):299–309.
32. Spaide RF, Fujimoto JG, Waheed NK. Image artifacts in optical coherence tomography angiography. *Retina*. 2015;35(11):2163–2180.
33. Maruko I, Koizumi H, Sawaguchi S, Hasegawa T, Arakawa H, Iida T. Choroidal blood vessels in retinal pigment epithelial atrophy using optical coherence tomography angiography. *Retin Cases Brief Rep*. Epub 2017 Jan 13.